TOTAL CROSS SECTION FOR HADRON PRODUCTION
BY ELECTRON-POSITRON ANNIHILATION BETWEEN
2.4 GeV AND 5.0 GeV CENTER-OF-MASS ENERGY*

J.-E. Augustin,[†] A. M. Boyarski, M. Breidenbach, F. Bulos,
J. T. Dakin,[‡] G. J. Feldman, G. E. Fischer, D. Fryberger, G. Hanson,
B. Jean-Marie,[†] R. R. Larsen, V. Lüth, H. L. Lynch, D. Lyon,
C. C. Morehouse, J. M. Paterson, M. L. Perl, B. Richter,
R. F. Schwitters, and F. Vannucci[‡]

Stanford Linear Accelerator Center
Stanford University, Stanford, California 94305

G. S. Abrams, D. Briggs, W. Chinowsky, C. E. Friedberg,
G. Goldhaber, R. J. Hollebeek,[††] J. A. Kadyk, G. H. Trilling,
J. S. Whitaker, and J. E. Zipse

Lawrence Berkeley Laboratory and Department of Physics
University of California, Berkeley, California 94720

ABSTRACT

The total cross section for hadron production by e^+e^- annihilation
has been measured at center-of-mass energies between 2.4 GeV and
5.0 GeV. Aside from the very narrow resonances $\psi(3105)$ and $\psi(3695)$,
the cross section varies between 32 nb and 17 nb over this region with
structure in the vicinity of 4.1 GeV.

We present measurements of the total cross section σ_T for hadron production by e^+e^- annihilation. Data were taken at 18 center-of-mass (c.m.) energies between 2.4 GeV and 5.0 GeV. These explorations, which contributed to the discovery of very narrow resonances in σ_T,[1] show further structure on a broader energy scale.

The experiment, performed at the SLAC electron-positron colliding beam facility, SPEAR,[2] used a solenoidal magnetic spectrometer to detect e^+e^- interactions. The properties of the SLAC/LBL magnetic detector and trigger requirements have been described previously.[3] Hadronic final states[4] were separated from e^+e^- and $\mu^+\mu^-$ final states by selecting events with ≥ 3 charged particles detected, unless two of the tracks were collinear within 10° and had large shower counter pulse height (consistent with electrons). Events with only two charged tracks were also classified hadronic if the tracks were acoplanar by more than 20°, and had small shower-counter pulse height (not electrons) and momenta ≥ 0.3 GeV/c. These 2-prong events constitute between 12% and 18% of the event sample.

The efficiency for hadrons to set the trigger system was determined from events with ≥ 3 charged particles. This efficiency is momentum dependent; it rises from 20% at 175 MeV/c to 80% at 450 MeV/c, then continues to rise slowly to 95% as the momentum increases.

Studies of radial vertex distributions and visual scanning of several thousand events showed that failures of the tracking to find an event vertex within a 4 cm radius cut lead to event losses which average 11% and do not favor any particular multiplicity or energy. The data were corrected for these losses.

The background due to beam-gas interactions was determined from longitudinal distributions of reconstructed event vertices. Runs taken with single beams have a uniform longitudinal distribution; colliding beam runs show, in

addition, a peak corresponding to the overlap region of the beams. The beam-gas background subtraction was <8% at all energies.

The contamination from photon-photon processes[5] was estimated using small angle (25 mrad) counters in coincidence with the detector to tag one or both of the forward angle electrons and positrons characteristic of these processes. The measured contamination of $\geq$ 3 prong hadron events (corrected for tagging efficiency) is 2 ± 2% at 4.8 GeV where the effect is expected to be largest. The tagging rate with two detected prongs is consistent with that calculated[6] for the electrodynamic processes $e^+e^- \rightarrow e^+e^- e^+e^-$, $e^+e^- \rightarrow e^+e^- \mu^+\mu^-$. To correct for that contamination, the number of two prong events was reduced by an amount ranging from 8% at the highest energy to 3% at the lowest. We estimate that less than 6% of the total hadron yield after corrections can be attributed to these photon-photon processes.

The efficiency for detecting multihadron final states was calculated in two steps. First, a computer simulation of the detector, incorporating all known inefficiencies, was combined with a model of hadronic states to compute the detection efficiency as a function of the number of charged particles in the final state. These efficiencies enter into an overdetermined set of simultaneous equations which relate true and observed charged-particle multiplicity distributions. The second step was to solve these equations for the true multiplicity distribution by a maximum likelihood method. The ratio of the number of events observed to that expected from the true distribution is the average detection efficiency $\bar{\epsilon}$. With this method, the form of the charged particle multiplicity distribution in the model does not directly enter into the determination of $\bar{\epsilon}$. Values for $\bar{\epsilon}$ and the true mean charged multiplicity as determined by this

procedure are given in the table. The errors on $\bar{\epsilon}$ and the mean multiplicity are statistical only.

The sensitivity of $\bar{\epsilon}$ to the choice of the model of multihadron production was checked by comparing three different models. In two models, angular and momentum distributions of particles were given by Lorentz invariant phase space. The third was a two-jet model where the jet axis had a $1 + \cos^2\theta$ or $\sin^2\theta$ angular distribution and particles decayed from each jet with transverse momentum spectra as observed in strong interactions. One phase-space model and the jet model assumed only pion production; the other phase-space model allowed for the production of kaons, etas, and nucleons in addition to pions. Values of $\bar{\epsilon}$ determined with these very different models agree to ± 5%.

Large angle Bhabha scattering $(e^+e^- \rightarrow e^+e^-)$ events were used to normalize the data. Procedures for selecting events and computing the integrated luminosity are discussed in Ref. 3. Integrated luminosities are presented in the table.

Radiative corrections[7] were applied by first subtracting the radiative tails of the two known ψ resonances[1] and then computing corrections due to the non-resonant cross section using the tail-subtracted cross section as input. These corrections range from - 6% to + 5%. The net radiative corrections, expressed as the ratio of measured cross sections to corrected ones, are given in the table.

Final values of σ_T are given in the table and Fig. 1a. The quoted errors include statistical errors to which an 8% systematic uncertainty was added in quadrature. This systematic error is an estimate of the point-to-point fluctuations which arise from errors in background subtraction, radial cut corrections, detection efficiency, and radiative corrections. It is consistent with the reproducibility of measurements taken under different operating conditions of the detector or separated by long periods of time.

A further, smooth variation in σ_T, as large as 15% from lowest energy to highest, could arise from systematic errors in the energy dependence of $\bar{\epsilon}$. To this must be added a 10% uncertainty in absolute normalization.

Aside from the narrow resonances indicated in Fig. 1a, the cross section falls smoothly with c.m. energy from 2.4 GeV to 3.8 GeV, where it rises sharply, peaking near 4.1 GeV before falling again. The radiative corrections which account for the tails of the ψ resonances (see table) make the 4.1 GeV peak more pronounced. In Fig. 1b, we present the ratio R of σ_T to the theoretical total cross section for production of muon pairs, together with earlier results from Frascati[8] and CEA.[9] R is approximately constant from 2.4 GeV to 3.8 GeV, rises between 3.8 and 4.1 GeV, and at 5 GeV has a value about twice that of the low energy "plateau". The structure shown in Fig. 1 suggests either new thresholds in the 4 GeV region or a broad resonance in σ_T centered at 4.1 GeV, or both.

While the present uncertainties in σ_T do not permit us to distinguish between these possibilities, we can estimate parameters describing this structure. Assuming it to be a single resonance above an 18 nb background, we find a peak centered at 4.15 GeV, an area of about 5500 nb-MeV, and a total width of 250 – 300 MeV. Further, assuming the resonance to have spin 1 (the one-photon state), we find a partial width to electrons of roughly 4 keV. The partial width to electrons is comparable to those of the $\psi(3105)$ and $\psi(3695)$ (approximately 5 keV, 2 keV, respectively[10]), while the total width is very much greater. No enhancement in the cross section for lepton pairs is observed near 4.1 GeV, nor is one expected because of the small branching ratio to leptons that this resonance would have.

REFERENCES

1. J.-E. Augustin et al., Phys. Rev. Letters 33, 1406 (1974); G.S. Abrams et al., Phys. Rev. Letters 33, 1453 (1974).

2. SPEAR Storage Ring Group, Proceedings of the IXth International Conference on High Energy Accelerators, Stanford Linear Accelerator Center (1974), pp. 37-42.

3. J.-E. Augustin et al., Phys. Rev. Letters, to be published (27 Jan. 1975).

4. σ_T presented here excludes all-neutral final states because of trigger requirements. The hadron nature of the particles can only be established in certain kinematic regions. K's and p's are unambiguously identified through time-of-flight below 600 MeV/c. Significant lepton contamination at intermediate momenta (0.1 GeV/c - 1.0 GeV/c) cannot be ruled out.

5. H. Terazawa, Rev. Mod. Phys. 45, 615 (1973).

6. Numerical integrations over the present detection system were performed using the differential cross sections of G. Grammer, Jr. and T. Kinoshita, Nucl. Phys. B80, 461 (1974).

7. G. Bonneau and F. Martin, Nucl. Phys. B27, 381 (1971); D.R. Yennie, Cornell Report No. CLNS-291 (1974); and Y.S. Tsai and D.R. Yennie (private communications).

8. $\gamma\gamma$ Group: C. Bacci et al., Phys. Letters 44B, 533 (1973); $\mu\pi$ Group: F. Ceradini et al., Phys. Letters 47B, 80 (1973); BCF Group: M. Bernardini et al., Phys. Letters 51B, 200 (1974).

9. A. Litke et al., Phys. Rev. Letters 30, 1189 (1973); G. Tarnopolsky et al., Phys. Rev. Letters 32, 432 (1974).

10. SLAC-LBL SPEAR collaboration, to be published.

TABLE

Center-of-Mass Energy $E_{c.m.}$ (GeV)	Integrated Luminosity L (nb)$^{-1}$	Average Detection Efficiency ϵ	Mean Charged Multiplicity $\langle n_{ch} \rangle$	Net Radiative Correction σ_{meas}/σ_T	Total Cross Section σ_T (nb)
2.4	26.1	0.40 ± 0.02	3.31 ± 0.12	1.02	31.8 ± 3.6
2.6	14.1	0.37 ± 0.03	3.18 ± 0.15	1.02	32.5 ± 4.4
2.8	14.9	0.38 ± 0.03	3.37 ± 0.18	1.02	29.4 ± 4.1
3.0	152.0	0.43 ± 0.01	3.55 ± 0.04	1.02	23.3 ± 2.0
3.1	16.7	0.40 ± 0.04	3.51 ± 0.21	1.02	22.5 ± 3.4
3.2	50.8	0.48 ± 0.02	3.89 ± 0.12	1.29	21.4 ± 2.3
3.3	22.7	0.47 ± 0.03	3.84 ± 0.19	1.17	18.9 ± 2.6
3.4	25.4	0.51 ± 0.03	3.93 ± 0.19	1.12	18.7 ± 2.4
3.6	33.4	0.52 ± 0.03	4.00 ± 0.17	1.07	19.1 ± 2.2
3.8	421.9	0.50 ± 0.01	3.87 ± 0.05	1.21	19.7 ± 1.7
4.0	18.3	0.52 ± 0.04	3.90 ± 0.20	1.03	24.5 ± 3.3
4.1	26.5	0.50 ± 0.03	4.04 ± 0.17	0.98	31.8 ± 3.6
4.2	70.5	0.51 ± 0.02	4.00 ± 0.10	1.02	28.1 ± 2.7
4.3	31.3	0.50 ± 0.03	4.02 ± 0.18	1.06	23.6 ± 2.8
4.4	21.3	0.58 ± 0.04	4.40 ± 0.24	1.08	19.6 ± 2.5
4.6	38.7	0.63 ± 0.04	4.62 ± 0.23	1.08	15.3 ± 1.9
4.8	787.2	0.58 ± 0.01	4.31 ± 0.04	1.05	18.2 ± 1.5
5.0	198.0	0.57 ± 0.02	4.32 ± 0.09	1.04	17.7 ± 1.5

FIGURE CAPTIONS

1a. Total hadronic cross section σ_T versus center-of-mass energy from this experiment. The positions of the narrow ψ resonances (Ref. 1) are indicated; their cross sections and radiative tails are not included in σ_T.

1b. Ratio R of σ_T to the theoretical muon pair production cross section versus $E_{c.m.}$. Also shown are previous results in the same energy region from Frascati (Ref. 8) and CEA (Ref. 9).
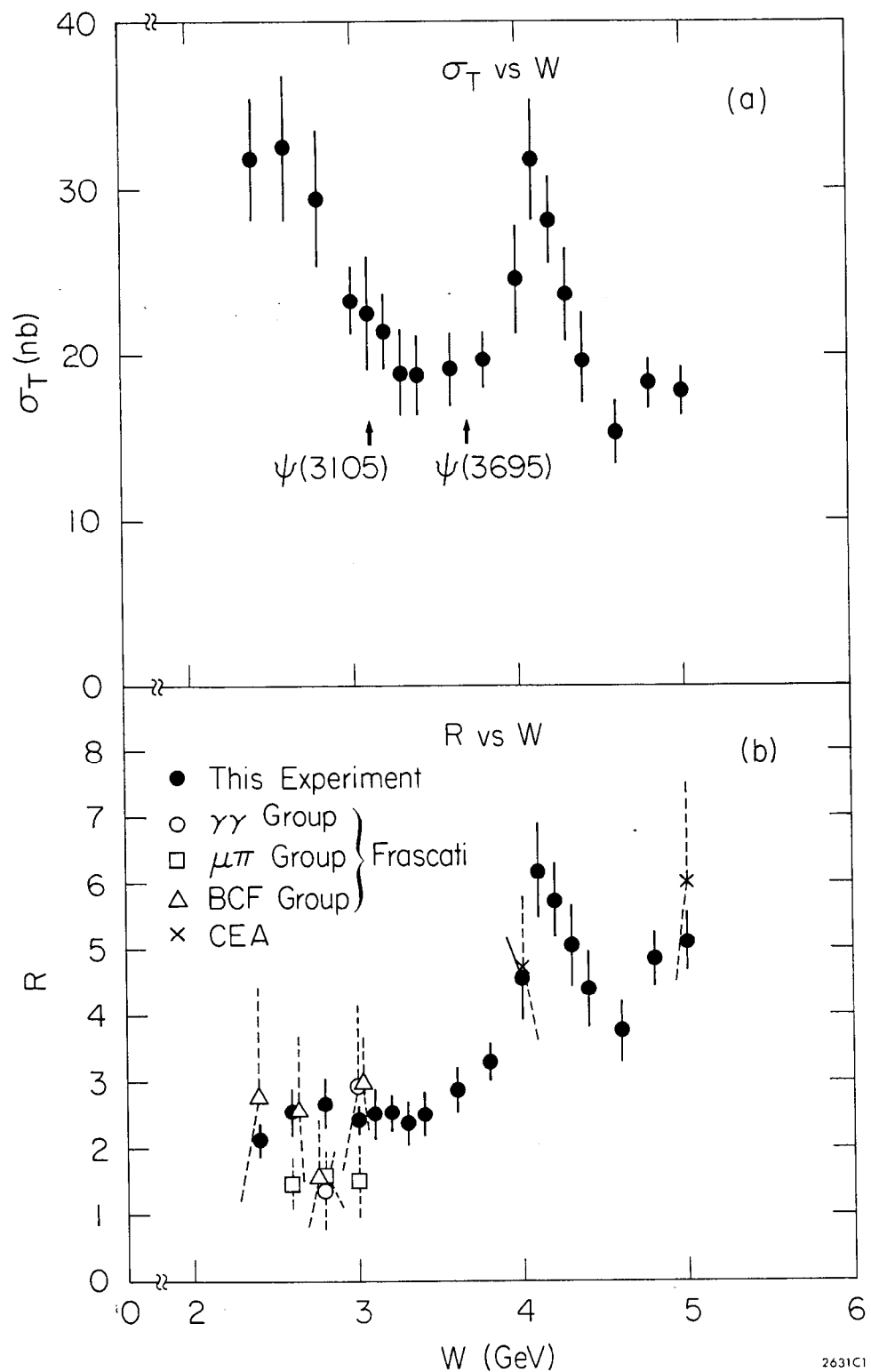
1a. Total hadronic cross section σ_T versus center-of-mass energy W from this experiment. The positions of the narrow ψ resonances (Ref. 1) are indicated; their cross sections and radiative tails are not included in σ_T.

1b. Ratio R of σ_T to the theoretical muon pair production cross section versus W. Also shown are previous results in the same energy region from Frascati (Ref. 8) and CEA (Ref. 9).